Article

Conformational Control of the Q to Q Electron Transfer in Bacterial Reaction Centers: Evidence for a Frozen Conformational Landscape below #25 °C

Nicolas Ginet*, and Je#ro#me Lavergne*

J. Am. Chem. Soc., **2008**, 130 (29), 9318-9331 • DOI: 10.1021/ja076504f • Publication Date (Web): 28 June 2008

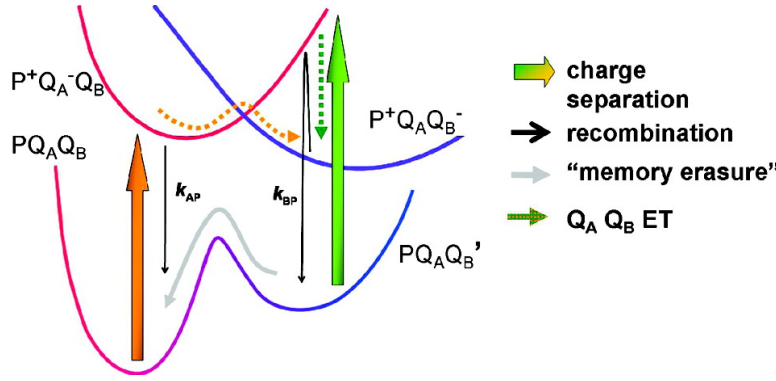

More About This Article

Additional resources and features associated with this article are available within the HTML version:

- Supporting Information
- Access to high resolution figures
- Links to articles and content related to this article
- Copyright permission to reproduce figures and/or text from this article

View the Full Text HTML

J|A|C|S
ARTICLES

Published on Web 06/28/2008

Conformational Control of the Q_A to Q_B Electron Transfer in Bacterial Reaction Centers: Evidence for a Frozen Conformational Landscape below −25 °C

Nicolas Ginet* and Jérôme Lavergne*

Laboratoire de Bioénergétique Cellulaire, iBEB, UMR 6191, CEA/CNRS and Université Aix-Marseille II, CEA Cadarache, 13108, Saint Paul lez Durance, France

Received August 29, 2007; E-mail: nicolas.ginet@cea.fr; jerome.lavergne@cea.fr

Abstract: The competition between the $P^+Q_A^-$ → PQ_A charge recombination (P, bacteriochlorophyll pair acting as primary photochemical electron donor) and the electron transfer to the secondary quinone acceptor $Q_A^-Q_B$ → $Q_AQ_B^-$ (Q_A and Q_B, primary and secondary electron accepting quinones) was investigated in chromatophores of *Rb. capsulatus*, varying the temperature down to −65 °C. The analysis of the flash-induced pattern for the formation of $P^+Q_AQ_B^-$ shows that the diminished yield, when lowering the temperature, is not due to a homogeneous slowing of the rate constant k_{AB} of the $Q_A^-Q_B$ → $Q_AQ_B^-$ electron transfer but to a distribution of conformations that modulate the electron transfer rate over more than 3 orders of magnitude. This distribution appears "frozen", as no dynamic redistribution was observed over time ranges > 10 s (below −25 °C). The kinetic pattern was analyzed to estimate the shape of the distribution of k_{AB}, showing a bell-shaped band on the high rate side and a fraction of "blocked" reaction centers (RCs) with very slow k_{AB}. When the temperature is lowered, the high rate band moves to slower rate regions and the fraction of blocked RCs increases at the expense of the high rate band. The RCs that recombine from the $P^+Q_AQ_B^-$ state appear temporarily converted to a state with rapid k_{AB}, indicating that the stabilized state described by Kleinfeld et al. (*Biochemistry* **1984**, *23*, 5780−5786) is still accessible at −60 °C.

Introduction

Biological electron transfer (ET) has generally been analyzed in terms of a nonadiabatic theory, where the protein movements coupled to ET are assumed to be thermally averaged on the relevant time scale. Recent works, often aimed at elucidating the effect of low temperatures[1−5] have proposed a different perspective, where conformational changes of the protein and solvent are not thermalized and play an active role in controlling the ET rate, so that the appropriate framework is that of the Sumi−Marcus[6] rather than Marcus[7] theory. These approaches come close to the studies on the functional role of protein dynamics developed by Frauenfelder and co-workers.[8] In the present paper, we analyze the temperature dependence of a reaction (the ET between the two quinone acceptors of the bacterial reaction center) that is known to be conformationally gated even at room temperature.[9] It turned out that, in this case, the range of conformations that exert the gating become immobilized at relatively high temperatures (−25 °C), allowing a detailed study of the conformation distribution and its temperature dependence.

Type 2 photosynthetic reaction centers (RCs), found in purple bacteria and in the photosystem II of cyanobacteria and chloroplasts, are characterized by the presence of two quinones, Q_A and Q_B, as electron acceptors. The photochemical charge separation results in the transfer of an electron from the primary donor P to Q_A in ∼200 ps, forming state $P^+Q_A^-$. The electron transfer to the secondary quinone Q_B occurs on a much slower time scale, by ∼5 orders of magnitude. In many purple bacteria (such as *Rhodobacter* (*Rb*) *sphaeroides* or *Rb. capsulatus*, used in the present work), the cofactors Q_A and Q_B are chemically identical, both ubiquinone-10 molecules. The protein matrix is thus responsible for the individualization of the two quinones. This concerns the strength of the association (Q_A is a permanent cofactor, whereas Q_B is exchangeable with the membrane-soluble quinone pool), the exergonic character of the electron transfer to Q_B, and the protonation reactions associated with Q_B reduction. The latter are probably responsible for the fact that Q_A is acting as a one-electron carrier, whereas Q_B is a "two-electron gate" undergoing two reduction steps. The Q_B cycle is summarized by the following reactions (see, for reviews, refs 10 and 11):

(1) Brettel, K. *Biochim. Biophys. Acta* **1997**, *1318*, 322–373.
(2) McMahon, B. H.; Müller, J. D.; Wraight, C. A.; Nienhaus, G. U. *Biophys. J.* **1998**, *74*, 2567–2587.
(3) Kotelnikov, A. I.; Ortega, J. M.; Medvedev, E. S.; Psikha, B. L.; Garcia, D.; Mathis, P. *Biolelectrochemistry* **2002**, *56*, 3–8.
(4) Kriegl, J. M.; Nienhaus, U. G. *Proc. Natl. Acad. Sci. U.S.A.* **2004**, *101*, 123–128.
(5) Wang, H.; Lin, S.; Allen, J. P.; Williams, J. C.; Blankert, S.; Laser, C.; Woodbury, N. W. *Science* **2007**, *316*, 747–750.
(6) Sumi, H.; Marcus, R. A. *J. Chem. Phys.* **1986**, *84*, 4894–4914.
(7) Marcus, R. A.; Sutin, N. *Biochim. Biophys. Acta* **1985**, *811*, 265–322.
(8) Frauenfelder, H.; Sligar, S. G.; Wolines, P. G. *Science* **1991**, *254*, 1598–1602.
(9) Graige, M. S.; Paddock, M. L.; Feher, G.; Okamura, M. Y. *Biochemistry* **1999**, *38*, 11465–73.
(10) Okamura, M. Y.; Paddock, M. L.; Graige, M. S.; Feher, G. *Biochim. Biophys. Acta* **2000**, *1458*, 148–163.
(11) Wraight, C. A. *Front Biosci.* **2004**, *9*, 309–337.

 10.1021/ja076504f CCC: $40.75

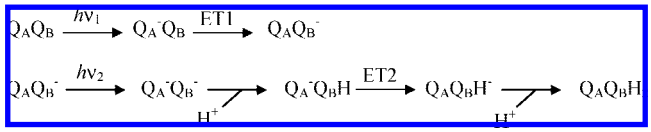

The first line depicts the photochemical reduction of Q_A followed by the "first electron transfer" ET1. The second line shows the reduction of the semiquinone Q_B^- to quinol Q_BH_2. The first event in this process is the protonation of the semiquinone Q_B^- to Q_BH, which permits the second ET reaction (ET2), followed by the second protonation.[9] The quinol can then leave the RC, allowing the binding to the Q_B pocket of an oxidized quinone from the lipid-soluble pool and the beginning of a new cycle.

It has been long known that both reduction reactions are not simple ET reactions, whose rate would depend on the driving force as predicted by Marcus theory.[7] This appears rather natural for the series of events described in the second line of the above scheme. But also, despite its apparently simpler mechanism, the first electron transfer was shown to be controlled by a conformational gating.[9,12] This expresses the fact that the reaction rate ($k_{AB} \approx (100\ \mu s)^{-1}$ in purified RCs) does not depend on the driving force, i.e., on the $-\Delta G_0$ (or ΔE_m) between Q_A and Q_B. However, a fast component with a time constant of 3−6 μs and amplitude depending on the material was also resolved, which showed the driving force dependence expected for a bona fide ET reaction.[13] The mechanism responsible for the gating is still unclear. Current models involve either a movement of the secondary quinone from a distal to a proximal binding site[14] or a progressive stabilization of Q_B^-, e.g., due to proton redistribution.[11,13]

In the present work, we investigate the effect of low temperatures on the $Q_A^-Q_B \rightarrow Q_AQ_B^-$ reaction in chromatophores of *Rb. capsulatus*. Previous studies of the effect of temperature on the recombination kinetics of the charge separated state $P^+Q_A^-$ in isolated RCs devoid of the secondary quinone have highlighted the role of conformational movements. The $P^+Q_A^-$ recombination in purple bacteria is a rare (unique?) example of a reaction which is not slowed but accelerated when lowering the temperature. Current explanations are based on the slowing of stabilization rearrangements (of the protein and solvent).[1,2,4,15] An appropriate framework for dealing with such processes where protein movements are not all thermally equilibrated in the relevant time scale is the Sumi−Marcus theory.[6] Besides the acceleration observed when lowering the temperature, the kinetics, which appear monoexponential at room temperature, become more heterogeneous. This phenomenon is dramatically enhanced when the system is frozen under illumination.[2,4] In line with studies from the Frauenfelder group on the binding of CO to myoglobin after photodissociation,[8,16] these results reveal the effect of freezing protein movements that exert a tight control on the kinetic processes studied. The apparent simplicity of the high temperature behavior reflects rapid averaging over the conformational manifold; when freezing or slowing these movements, the role of the protein dynamics is expressed as a broad dispersion of the kinetic rates. It is of interest in this perspective to analyze the behavior at low temperature of the conformationally gated $Q_A^-Q_B \rightarrow Q_AQ_B^-$ reaction.

In the absence of a secondary donor to the RC, the electron of Q_A^- is subject to a competition between two routes, i.e., the transfer to the secondary quinone and the recombination with the oxidized primary donor P^+ (P is a bacteriochlorophyll pair acting as primary photochemical electron donor). When lowering the temperature, the latter route becomes predominant because of the slower transfer to Q_B, while the recombination reaction is accelerated at low temperature. This competition can be studied by monitoring the kinetics of P^+ decay, which can be obtained in a sensitive manner through the changes of the yield of bacteriochlorophyll fluorescence.

Experimental Section

The FJ2 strain of *Rb. capsulatus* (a kind gift of Prof. F. Daldal) was derived from a green strain (MT1131) and deleted in both cytochrome c_2 and the alternative membrane-bound cytochrome c_y.[17] Chromatophores were prepared as previously described.[18] They were stored at −80 °C in a medium containing 20% glycerol (v/v). For the experiments, the chromatophores were diluted 5 times in a Tris (50 mM, pH 8), KCl (50 mM) buffer, thus containing a final concentration of 4% glycerol. Alternatively, when mentioned, the medium contained 66% glycerol (v/v). Both situations will be subsequently referred to as "low" and "high" glycerol.

The experiments were carried out using the apparatus described by Joliot et al.[19] This version of the Joliot−Béal flash spectrophotometer [20,21] was adapted to measurements of light-induced changes at temperatures between +35 and −65 °C. The absorption is sampled using 2 μs monochromatic flashes given at various intervals after the actinic excitation. To adapt this technique to low-temperature measurements, the biological material is placed in measuring and reference cuvettes 0.2 mm thick (1.3 cm^2 area); the rear face of each cuvette is formed by a polished aluminum plate that reflects actinic and detecting light. A Peltier device is glued on the rear face of the aluminum plate and allows the adjustment of the temperature of the sample, which is measured through a thermocouple inserted within the aluminum plate.

The machine lends itself to absorption or fluorescence measurements. In the latter case, the fluorescence excited by the detection flashes at 450 nm is measured through a Wratten 89B filter. The actinic illumination consisted either of saturating xenon flashes filtered through a Schott BG39 or continuous 875 nm light of adjustable intensity from a 875 nm LED array. The synchronous detection of the fluorescence excited by the detection flashes could be carried out even during the 875 nm actinic illumination, except when its intensity was too high. The individual energy fluctuations of the detection flashes were corrected using a measurement on a reference path. In this manner, the intensity of the fluorescence flashes is proportional to the emission yield of the sample. Under the conditions used in this work (no electron donor to the RC), the bacteriochlorophyll fluorescence yield Φ is modulated by the amount of RCs in the closed state P^+; the ratio between the maximum level (100% P^+) and the dark-adapted level (100% P) is ∼3.5. However, due to the fact that several RCs share a common antenna of light-harvesting complexes, the relationship

(12) Graige, M. S.; Feher, G.; Okamura, M. Y. *Proc. Natl. Acad. Sci. U.S.A.* **1998**, *95*, 11679–11684.
(13) Li, J.; Takahashi, E.; Gunner, M. R. *Biochemistry* **2000**, *39*, 7445–7454.
(14) Stowell, M. H. B.; McPhillips, T. M. D.; Rees, D. C.; Soltis, S. M.; Abresch, E.; Feher, G. *Science* **1997**, *276*, 812–816.
(15) Ortega, J. M.; Mathis, P.; Williams, J. C.; Allen, J. P. *Biochemistry* **1996**, *35*, 3354–3361.
(16) Ansari, A.; Berendzen, J.; Bowne, S. F.; Frauenfelder, H.; Iben, I. E. T.; Sauke, T. B.; Shyamsunder, E.; Young, R. D. *Proc. Natl. Acad. Sci. U.S.A.* **1985**, *82*, 5000–5004.
(17) Jenney, F. E.; Daldal, F. *EMBO J.* **1993**, *12*, 1283–1292.
(18) Lavergne, J.; Matthews, C.; Ginet, N. *Biochemistry* **1999**, *38*, 4542–4552.
(19) Joliot, P.; Joliot, A.; Verméglio, A. *Biochim. Biophys. Acta* **1997**, *1318*, 374–384.
(20) Joliot, P.; Béal, B.; Frilley, B. *J. Chim. Phys.* **1980**, *77*, 209–216.
(21) Joliot, P.; Joliot, A. *Biochim. Biophys. Acta* **1984**, *765*, 210–218.

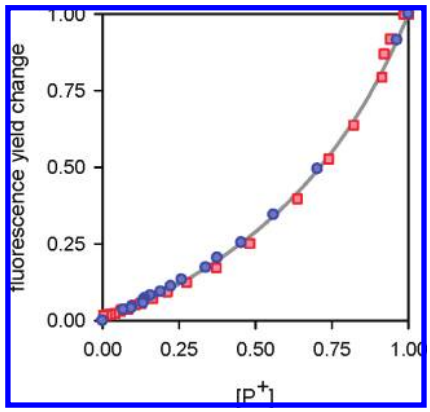

Figure 1. Plot of the normalized variable fluorescence yield against the fraction of P^+ (monitored as the absorption change at 603 nm). Both changes were recorded at the same discrete times after a saturating flash, during the recombination process (involving essentially the decay of $P^+Q_B^-$ at high temperature, and also the phase corresponding to $P^+Q_A^-$ recombination at low temperature, as explained in the text). The data were obtained at +20 °C (red squares) and −50 °C (blue circles). The line is a fit as explained in the text.

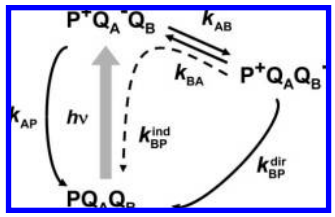

Figure 2. Scheme depicting charge separation and electron transfer in RCs in the absence of a secondary electron donor. The yield of $P^+Q_AQ_B^-$ formation depends on the competition between electron transfer to Q_B (k_{AB}) and recombination from $P^+Q_A^-$ (k_{AP}). The recombination from $P^+Q_AQ_B^-$ (with overall rate constant $k_{BP} = k_{BP}^{dir} + k_{BP}^{ind}$) involves two competing pathways, direct (k_{BP}^{dir}) and indirect (k_{BP}^{ind}; dashed arrow).

between Φ and the fraction $[P^+]$ of closed RCs is not linear but hyperbolic.[22–24] This is shown in Figure 1, where the variable fluorescence Φ_v (obtained by subtracting from Φ the dark-adapted level Φ_Φ) was plotted against an absorption change (603 nm) reflecting the amount of P^+. Both quantities were recorded, using the same timing of detection flashes, during the recombination reaction ($P^+Q_B^- \rightarrow PQ_B$) after a saturating flash. The data were fitted by the function $\Phi_v = [P^+]/(1 + J - J \times [P^+])$, where J is an adjustable parameter expressing the excitonic connectivity. We found that the dependence of Φ_v as a function of $[P^+]$ was the same over the whole temperature range explored in this study, with $J \approx 1.45$, as illustrated in Figure 1, showing data at +20 and −50 °C. This relationship was then routinely used to convert fluorescence changes in terms of $[P^+]$.

Results

Electron Transfer and Recombination Scheme. The *Rb. capsulatus* strain FJ2 used in this study has undergone genetic deletion of the two cytochromes that act as physiological electron donors to the photochemical bacteriochlorophyll pair P on the RC.[17] The scheme of Figure 2 shows the various electron transfer reactions that may follow the photochemical production of state $P^+Q_A^-$. A first route of $P^+Q_A^-$ decay is charge recombination to the ground-state PQ_A. In RCs where

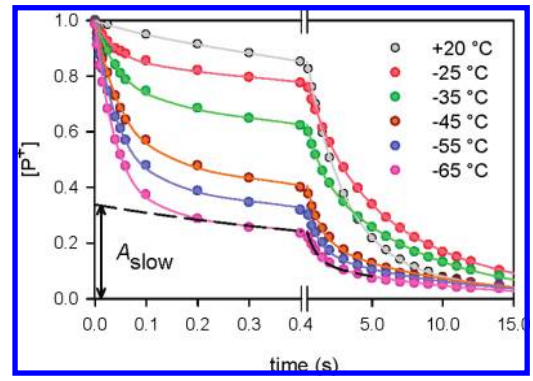

Figure 3. P^+ reduction kinetics between +20 and −65 °C. The kinetic data (shown here for the low glycerol medium) were fitted with a sum of three exponentials (lines). The fast phase, with $t_{1/2}$ in the 25−45 ms range, reflects the initial competition between ET to Q_B and $P^+Q_A^-$ recombination. A_{slow} is the sum of the two slower phases and corresponds to the yield of $P^+Q_AQ_B^-$ formation.

Q_A is a ubiquinone, such as *Rb. capsulatus*, this process takes place by direct tunneling from Q_A^- to P^+; the half-time of this process in FJ2 chromatophores is ∼45 ms at room temperature. This is of course much slower than the electron transfer $Q_A^-Q_B \rightarrow Q_AQ_B^-$, which occurs, in this material, with $t_{1/2} \approx 30$ μs (data not shown). The state $P^+Q_AQ_B^-$ thus formed can return to the ground state through two competing reactions: direct tunneling from Q_B^- to P^+; or the indirect pathway whereby the recombination step occurs from $P^+Q_A^-$, after the uphill jump of the electron from Q_B^- to Q_A. This is actually the predominant route, with $t_{1/2} \approx 1.9$ s (in FJ2 chromatophores, pH 8, at +20 °C), while the direct pathway is ∼5-fold slower.[18,25]

In agreement with this kinetic pattern, the reduction of P^+ after a saturating flash at room temperature is almost entirely due to $P^+Q_B^-$ recombination. However, when lowering the temperature (Figure 3), a faster component is observed, whose relative amplitude increases as T decreases. This has been ascribed to the slowing of the $Q_A^-Q_B \rightarrow Q_AQ_B^-$ reaction,[26–28] so that the $P^+Q_A^-$ recombination is now efficiently competing. In the temperature range investigated in Figure 3, the P^+ decay can be fitted as a sum of three exponentials. The fast component has increasing amplitude as the temperature is lowered and corresponds to the $P^+Q_A^-$ decay competing with the electron transfer to Q_B. The slower components, with $t_{1/2}$ values of a few hundreds of milliseconds to a few seconds, correspond to $P^+Q_B^-$ recombination: their combined amplitude is denoted as A_{slow}. Although it gave satisfactory fits, the decomposition of the latter process as a sum of two exponentials may have no real significance, and a broader rate distribution could in fact be more adequate (for example, good fits of the $P^+Q_A^-$ recombination kinetics were obtained using both descriptions, see refs 2 and 29).

(22) Vredenberg, W. J.; Duysens, L. N. M. *Nature* **1963**, *197*, 355–357.
(23) Lavergne, J.; Trissl, H. W. *Biophys. J.* **1995**, *68*, 2474–2492.
(24) Comayras, F.; Jungas, C.; Lavergne, J. *Biophys. J.* **2005**, *280*, 11203–11213.
(25) Labahn, A.; Bruce, J. M.; Okamura, M. Y.; Feher, G. *Chem. Phys.* **1995**, *197*, 355–366.
(26) Chamorovsky, S. K.; Rememnikov, S. M.; Kononenenko, A. A.; Venediktov, P. S.; Rubin, A. B. *Biochim. Biophys. Acta* **1976**, *430*, 62–70.
(27) Kleinfeld, D.; Okamura, M. Y.; Feher, G. *Biochim. Biophys. Acta* **1984**, *766*, 126–140.
(28) Xu, Q.; Gunner, M. R. *Biochemistry* **2001**, *40*, 3232–3241.
(29) Schoepp, B.; Parot, P.; Lavorel, J.; Verméglio, A. In *The Photosynthetic Bacterial Reaction Center II*; Breton, J., Verméglio, A., Eds; NATO ASI Series; Plenum Press: New York, 1992; pp 331−339

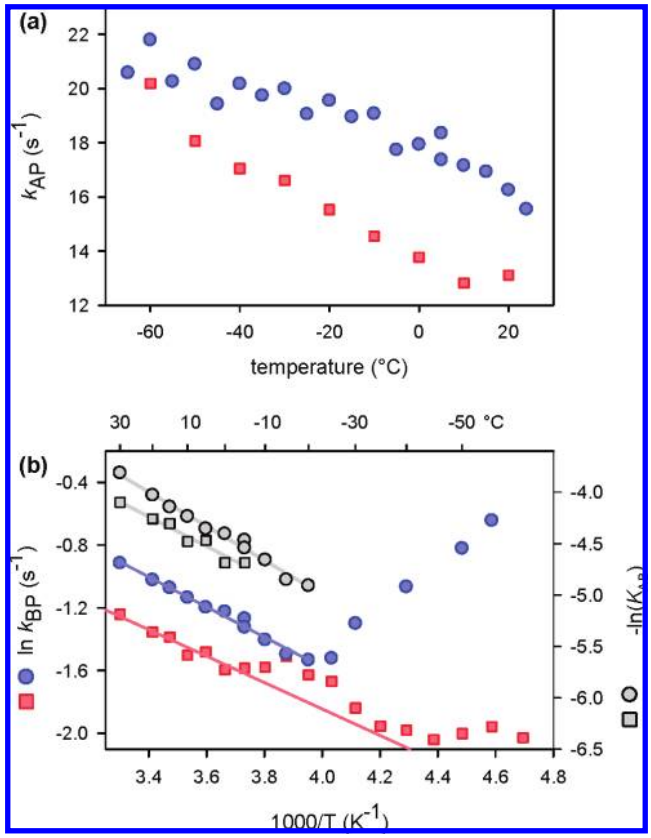

Figure 4. Recombination rates as a function of temperature. The blue circles and red squares refer to experiments in the low and high glycerol media, respectively. (a) A direct plot of k_{AP} vs T. k_{AP} was obtained from a single exponential fit of the recombination kinetics in the presence of 10 μM stigmatellin. (b) An Arrhenius plot of ln(k_{BP}) vs 1/T. The gray lines and symbols (using the vertical scale on the right) show the van't Hoff plot: $-\ln(K_{AB}) = -\ln(k_{AP}/(k_{BP} - k_{BP}^{dir}) - 1) = f(1/T)$.

Before proceeding to our major topic, which is to analyze the competition between the $P^+Q_A^-$ recombination and the ET to Q_B, we shall first examine how the individual rates of the two recombination processes vary with T.

Temperature Dependence of the Recombination Rates. The recombination kinetics of $P^+Q_A^-$ can be determined from the flash-induced changes of the fluorescence yield in chromatophores in the presence of stigmatellin as an inhibitor of Q_B reduction. The P^+ reduction follows monoexponential kinetics from which the k_{AP} rate constant was determined (a small slow phase in the seconds time range, due to uninhibited RCs, was also taken into account in the kinetic analysis). The room temperature rate in FJ2 chromatophores ($t_{1/2} \approx 45$ ms) is similar to that found in chromatophores from *Rb. sphaeroides* ($t_{1/2} \approx$ 47 ms),[30] which is significantly faster than that in isolated RCs ($t_{1/2} \approx 80-100$ ms). One may also notice that the recombination kinetics in *Rb. capsulatus* chromatophores remain monophasic down to (at least) −60 °C, whereas, in *Rb. sphaeroides* RCs, a significant heterogeneity is observed at this temperature (and becomes more pronounced at lower temperature).[2,29]

A (direct) plot of k_{AP} vs T is shown in Figure 4a, with chromatophores suspended in buffers with 4% (v/v) glycerol (residual from the storage medium) or with 66% glycerol. Over the temperature range explored in these experiments the recombination is slightly slower in the high glycerol medium compared with the low glycerol medium ($t_{1/2}$ of 53 and 43 ms at +20 °C, respectively). The low glycerol medium was frozen below 0 °C, but this caused no obvious effect on the $P^+Q_A^-$ recombination rate.

The temperature dependence of the $P^+Q_B^-$ recombination was analyzed from data such as those of Figure 3. As noticed above, the kinetics are multiphasic: for simplicity, we used the overall half-time of the decay (excluding the $P^+Q_A^-$ recombination phase) as an indicator of the "average" rate, and the rate constant k_{BP} used in Figure 4b was accordingly computed as ln(2)/$t_{1/2}$. The heterogeneity of the $P^+Q_B^-$ decay curves at subzero temperatures was more pronounced in the low glycerol medium, while in the high glycerol medium the decay was closer to a single exponential. For instance, at −50 °C, the decomposition gives (excluding the $P^+Q_A^-$ recombination phase) 43% ($t_{1/2} \approx$ 550 ms) and 57% ($t_{1/2} \approx 7$ s) in the low glycerol medium and 19% ($t_{1/2} \approx 1$ s) and 81% ($t_{1/2} \approx 7.5$ s) in the high glycerol medium.

According to the scheme of Figure 1, one expects that $k_{BP} = k_{AP}/(1 + K_{AB}) + k_{BP}^{dir}$, where K_{AB} is the electron transfer equilibrium constant between Q_A and Q_B. This behavior is verified in the high temperature range. The gray symbols and lines in Figure 4b show, for both types of solvent, van't Hoff plots $\ln(K_{AB}) = f(1/T)$, with K_{AB} computed from the above expression. In this manner one estimates for the enthalpy differences ($Q_B - Q_A$): $\Delta H_{AB} = -143$ meV (low glycerol) and −125 meV (high glycerol); the entropy differences ΔS_{AB} are −0.14 meV K^{-1} and −0.058 meV K^{-1}, respectively. At +20 °C, this corresponds to $\Delta G_{AB} = -102$ and −108 meV, respectively (using this procedure in isolated RCs of *Rb. sphaeroides*, Mancino and co-workers obtained $\Delta G_{AB} = -71$ meV).

Tentatively, the effects of glycerol on the Q_A/Q_B equilibrium may be rationalized as due to the decrease of the solvent polarity while assuming that the interaction of Q_B^- with the aqueous medium exceeds that of Q_A^-. This could account for the fact that $S_B < S_A$, because of the greater dielectric ordering of the solvent around Q_B^-. A decreased polarity of the medium should then imply a lesser enthalpic stabilization of Q_B^- with respect to Q_A^- and an opposite entropic effect, as was indeed found. Both effects almost cancel out at room temperature, and the main reason for the slower k_{BP} in the high glycerol medium is the slower k_{AP}, an effect for which we found no obvious explanation.

In the low glycerol medium (blue symbols in Figure 4b), the data for $P^+Q_B^-$ recombination deviate wildly from the Arrhenius behavior below −20 °C. This is well below the freezing point of the medium (when cooling the sample, the freezing was observed between −5 and −10 °C due to supercooling; when raising T, thawing occurred close to 0 °C). Below −20 °C, the overall recombination rate increased and became more heterogeneous, as noted above. This phenomenon was not observed in the 66% glycerol medium, where the rate continued to slow down with approximate Arrhenius behavior down to −40 °C, where a plateau was reached. This indicates the switch to the regime where the direct recombination pathway becomes predominant. The plot displays a bump in the −10 to

(30) Ginet, N.; Lavergne, J. *Biochemistry* **2000**, *39*, 16252–16262.
(31) Mancino, L. J.; Dean, D. P.; Blankenship, R. E. *Biochim. Biophys. Acta* **1984**, *764*, 46–54.

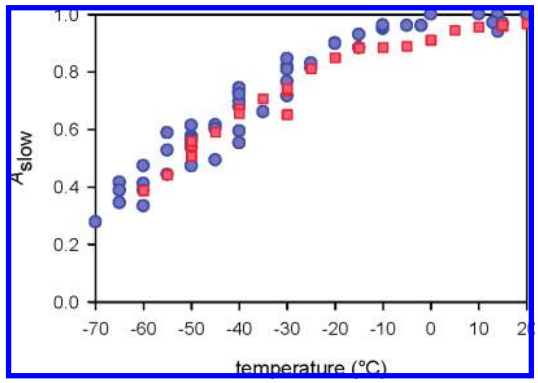

Figure 5. Dependence on temperature of the yield of $P^+Q_B^-$ formation on a saturating flash, A_{slow}, in the low (blue circles) and high (red squares) glycerol media.

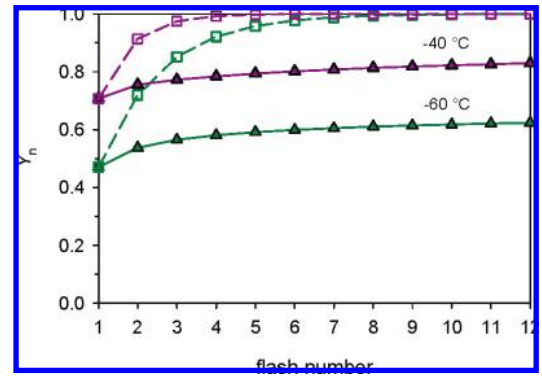

Figure 6. A comparison of the experimental Y_n pattern (closed symbols) with simulations assuming homogeneity of the RC population (open symbols). Chromatophores in the low glycerol medium were subjected to a series of saturating flashes 200 ms apart, at −40 and −60 °C. Data were sampled 100 ms after each actinic flash (this is a good approximation for A_{slow} as defined in Figure 3). The simulated patterns, assuming that all RCs have the value of ρ corresponding to Y_1, were computed with eq 2.

−30 °C range; this feature, of unknown origin, is above the noise level and was consistently observed.

The yield of $P^+Q_B^-$ formation decreases when lowering the temperature Based on the scheme of Figure 2, one expects the relative amplitude of the slow recombination phase (from $P^+Q_B^-$) to be

$$A_{slow} = \frac{k_{AB}}{k_{AB} + k_{AP}} \equiv \rho \qquad (1)$$

Here, ρ is defined as the probability of the Q_A^- electron to be transferred to Q_B. The dependence of A_{slow} (as defined in Figure 3) on T is presented in Figure 5, for the low and high glycerol media. The $A_{slow}(T)$ relation was found independent of the direction of the temperature changes. When switching the temperature as rapidly as allowed by our setup between −50 and −60 °C (this took about 17 s), we found no measurable delay between the attainment of the new temperature and the response of the sample for the measurement of A_{slow} after one flash: this sets the time constant for the sample response below ~20 s. The $A_{slow}(T)$ results shown in Figure 5 are very similar to those reported by Xu and Gunner,[28] obtained with isolated RCs from *Rb. sphaeroides* (in the presence of 66% glycerol). The latter authors used eq 1 to retrieve the k_{AB} rate as a function of T and thence estimate the activation enthalpy and entropy of this reaction. This analysis is based on the assumption that the system is reasonably homogeneous, so that the k_{AB} estimated in this manner retains a physical meaning. It was however pointed out by Tiede et al.[32] that, at −22 °C, the electron transfer appeared already broadly distributed in time (i.e., spanning the 1 μs−20 ms time range). In the following, we shall confirm and further characterize this heterogeneous behavior.

Heterogeneous Distribution of ρA simple test for the homogeneity of the system is to analyze the effect of a train of saturating flashes. If the time interval between the flashes is ~100 ms, such that the $P^+Q_A^-$ recombination is almost terminated while the $P^+Q_B^-$ has barely started, one expects the accumulation of Q_B^- to follow a progression of the following form:

$$y(n, \rho) = 1 - (1 - \rho)^n \qquad (2)$$

Here, y is the fraction of Q_B^- accumulated after the n-th flash. This expression can be obtained, e.g., by noticing that the probability that a RC fails n times to yield Q_B^- is $(1 - \rho)^n$. This predicts a rapid progression; assuming for instance $\rho = 0.5$ (as is apparently the case for $T \approx -55$ °C), one should observe successively 0.5, 0.75, 0.875, 0.938. As shown in Figure 6, this prediction is markedly at odds with the experimental results (that we denote as Y_n), which show a much smaller and slower progression. The observed behavior (the solid triangles show data obtained at −60 and −40 °C) is clearly inconsistent with a homogeneous model (open squares) and suggests that, at each temperature, some fraction of the RCs has a high probability to produce Q_B^- (i.e., $\rho \approx 1$), while the other fraction has a low ρ. Furthermore, for the temperatures shown here, the fraction of RCs that has a ρ value close to the mean (the mean value $\langle\rho\rangle$ is given by Y_1, the A_{slow} value after the first flash) must be small. Taking for instance the −60 °C data, one has $\langle\rho\rangle \approx 0.47$. The contribution of the RCs for which $\rho = 0.47$ to the increment on the second flash ($Y_2 - Y_1$) is $\rho(1 - \rho) \approx 0.25$. The increment actually observed is $Y_2 - Y_1 \approx 0.067$. If this was entirely due to RCs with $\rho \approx 0.47$, the amount of such RCs would be $0.067 \times 0.25 \approx 0.017$. Thus the data imply that less than 1.7% of the RCs have ρ close to the mean value 0.47. This qualitative argument shows that the distribution of ρ must be quite broad.

Frozen Landscape or Conformational Equilibrium? Having recognized the heterogeneous character of the system, the question arises of the dynamics of this heterogeneous distribution: are we dealing with an essentially "frozen" system, or is there a measurable interconversion rate between RCs with small and large values of ρ? One may reason that, in the latter case, it should be possible to accumulate a larger fraction of RCs in the $P^+Q_B^-$ state by prolonging the illumination: whenever low ρ RCs are converted to high ρ, the illumination will collect them into the $P^+Q_B^-$ "trap". Furthermore, the rate of the accumulation of $P^+Q_B^-$ under prolonged illumination of sufficient intensity should be limited by the rate of the conformational equilibrium. From this perspective, we examined the behavior of our chromatophores at low temperature when submitted to continuous illumination of variable intensity or to a train of saturating flashes with variable time spacing (Δt), as illustrated in Figure 7. These experiments show that one does observe a progressive accumulation of RCs in the $P^+Q_B^-$ state under prolonged illumination. They also reveal, however, that the time course of this process is under photochemical control and does not show the intensity-independent limiting rate expected for a confor-

(32) Tiede, D. M.; Vasquez, J.; Cordova, J.; Marone, P. A. *Biochemistry* **1996**, *35*, 10763–10775.

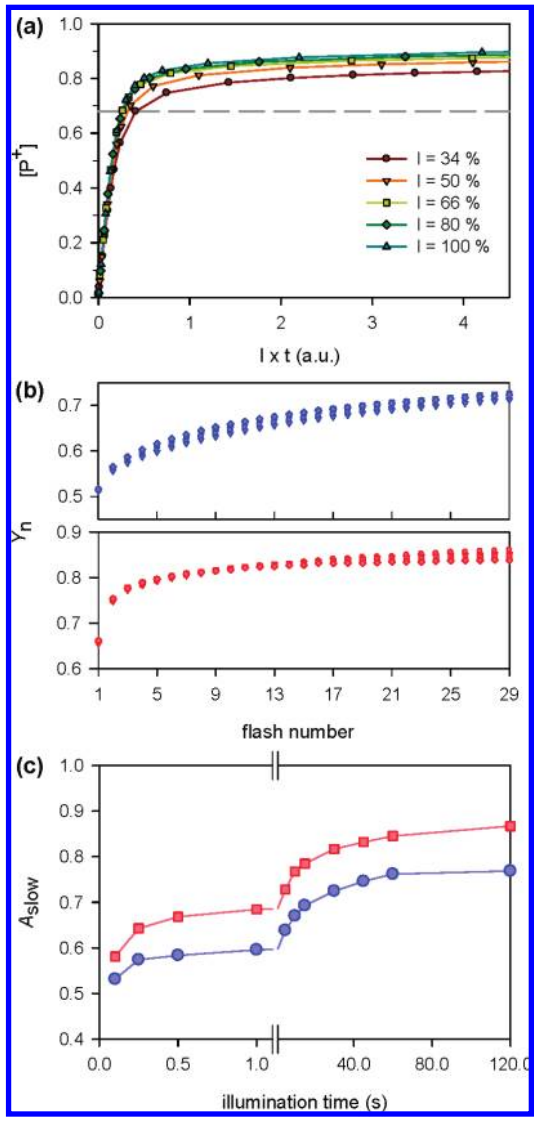

Figure 7. Tests for deciding between alternative interpretations of the ρ heterogeneity (frozen landscape or conformational equilibrium). (a) Time course of P^+ accumulation under continuous 875 nm illumination of variable intensity (using neutral density filters with transmittance as indicated; the 100% intensity is arbitrary). In this intensity range, the photochemical rate is slow with respect to k_{AP}, so that the amount of P^+ formed corresponds approximately to $P^+Q_AQ_B^-$. The horizontal scale is the product time × transmittance. The experiment was run at −40 °C in the low glycerol medium. (b) The Y_n pattern in the low (blue symbols, top panel) and high (red symbols bottom panel) glycerol media, at −40 °C. The samples were subjected to a series of 30 actinic flashes with variable time spacing (circles, 100 ms; triangles, 200 ms; squares, 300 ms; diamonds, 400 ms). The data show the amount of P^+ sampled at 100 ms after each flash, which is a good approximation for A_{slow} (see Figure 3). (c) Kinetics of $P^+Q_AQ_B^-$ accumulation at −50 °C under a saturating illumination. Pulses of saturating 875 nm light of variable duration were shone on the sample and the decay kinetics were recorded after shutting the light off, allowing the determination of A_{slow} (i.e., the amount of $P^+Q_AQ_B^-$). The blue and red symbols indicate the use of the low and high glycerol media.

mational relaxation. This point is apparent in the intensity × time plots shown in Figure 7a. The intensities used in this experiment were in the range where the photochemical turnover is relatively fast with respect to $P^+Q_B^-$ recombination and slow with respect to $P^+Q_A^-$ recombination, so that the observed level of P^+ reflects roughly the amount of $P^+Q_B^-$. The dashed gray line indicates the level reached after one saturating flash. The slow phases after the rapid rise to this level have similar kinetics in the $I \times t$ plot, over a 2-fold intensity change. For lower intensities, the P^+ level is depressed because of the $P^+Q_B^-$ recombination. A still more clear-cut situation is found when using saturating flashes with variable time spacing. Figure 7b shows the result of an experiment, plotting the P^+ level sampled 100 ms after each flash, for Δt between flashes ranging from 100 to 400 ms. The horizontal scale is the flash number, thus covering a time lapse extending from 3 to 12 s. The data for the various values of Δt are almost superimposed, showing that, in this time domain, the accumulation of $P^+Q_B^-$ is strictly dependent on the number of photochemical turnovers, involving no "dark" reaction such as conformational relaxation. The pure flash number dependence of $P^+Q_B^-$ accumulation was verified at all temperatures in the −25 to −60 °C range (−25 °C is approximately the highest temperature at which the test can be run accurately because at higher temperature the amplitude of the changes is small, as A_{slow} is close to 1, Figure 5). In the high glycerol medium (lower panel in Figure 7b) this behavior was also verified. However, a small but systematic deviation can be noticed on the slower phases, which are slightly clipped when increasing the flashing interval. The reason for this effect will be discussed later.

We pursued this investigation by testing the effect in the low temperature region of pulses of DC light of saturating intensity (i.e., with a photochemical rate much faster than the rate of $P^+Q_A^-$ recombination). After a pulse of variable duration, the amount of $P^+Q_B^-$, plotted in Figure 7c, was determined from the A_{slow} of the decay kinetics. Under such conditions, the level reached after a pulse of 500 ms is close to the level reached after a train of 20−30 saturating flashes: this is consistent with the fact that the saturating DC pulse induces photochemical turnovers (in the fraction of centers which are not in the $P^+Q_B^-$ state) at a rate limited by the $P^+Q_A^-$ recombination, with $k_{AP} \approx 21\ s^{-1}$. A slow rise of $P^+Q_B^-$ is then observed for longer illumination times, with, at $T = -50$ °C, $t_{1/2} \approx 12$ s in both the low and high glycerol media. This phase is probably a continuation of the stochastic photochemical process due to RCs with small but nonzero ρ. For a photochemical rate of $21\ s^{-1}$, a rise with $t_{1/2} \approx 12$ s corresponds to an average ρ of ∼0.003. It is unlikely that this phase is due to a conformational relaxation (i.e., RCs escaping the low ρ conformations) because this would have affected the flash experiments (panel b) run in this time range. When the 12 s phase is completed, there remains a quite significant fraction of RCs (12% and 23% in the high and low glycerol media, respectively), which have still not been able to reach the $P^+Q_B^-$ state after 120 s of saturating illumination.

***P*(ρ,*T*) Distribution.** We are thus led to a "frozen landscape" picture, where the distribution of the ρ values (the yield of $P^+Q_B^-$ formation) at each temperature below −25 °C (at least) appears fixed over a time range of more than 10 s (and actually more than several minutes at −50 °C as inferred from the experiment of Figure 7c). A fixed distribution $P(\rho,T)$ accounts for the "pure flash number dependence" feature, because it predicts that the accumulation of $P^+Q_B^-$ is based on eq 2, i.e.:

$$Y_n = \int_0^1 P(\rho)\, y(n,\rho)\, d\rho \qquad (3)$$

(omitting the T parameter). One should keep in mind, however, that eqs 2 and 3 account for a somewhat idealized situation, assuming that the recombination of $P^+Q_A^-$ is complete between two successive flashes and that of $P^+Q_B^-$ is unstarted. With $\Delta t = 200$ ms, the first assumption is verified (with $t_{1/2} \approx$ 35 ms, the $P^+Q_A^-$ recombination is 98% complete), but the

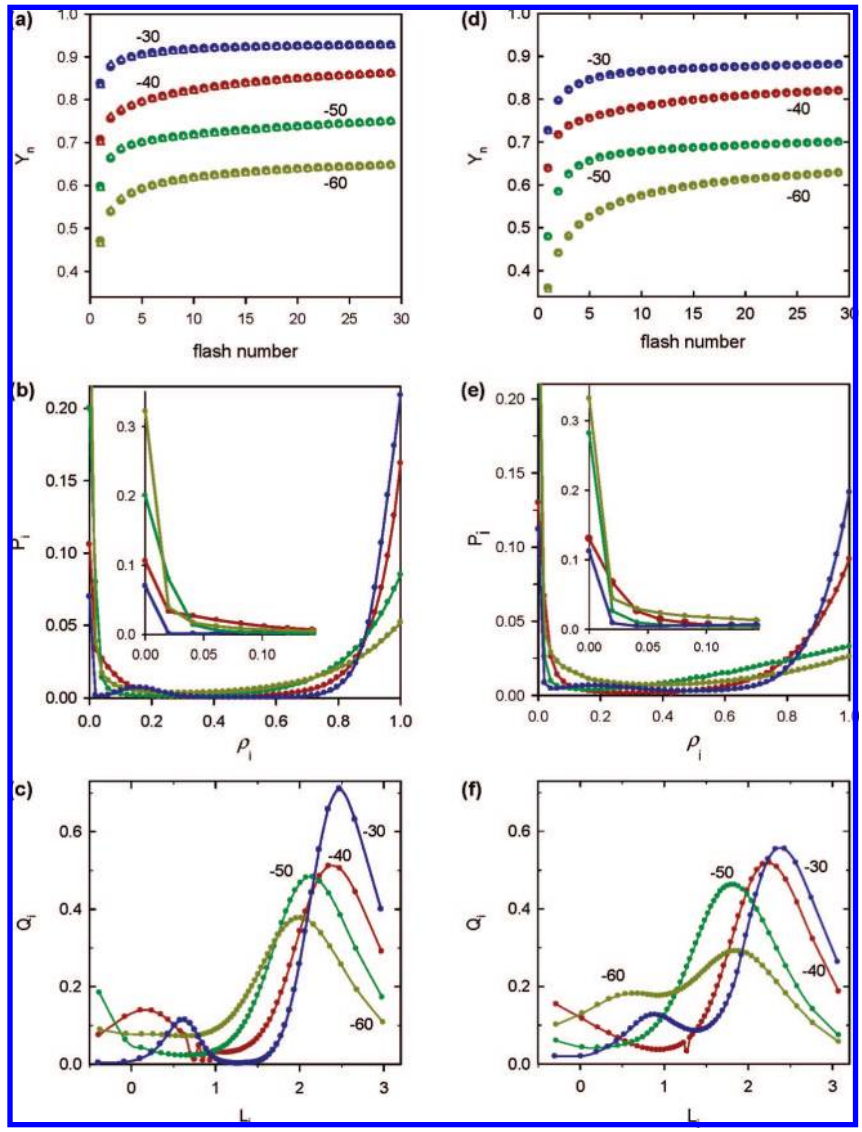

Figure 8. Experimental Y_n series and calculated distributions of ρ and $\log(k_{AB})$ at different temperatures, as indicated. The left- and right-hand panels show the results obtained in the low and high glycerol media, respectively. (a and d): The full circles show the experimental data (obtained by measuring P^+ at 100 ms after each flash of a series with 200 ms spacing; a small correction, estimated independently from the decay kinetics, was applied to restore the value of A_{slow}). The open triangles (generally superimposed on the data) show the results of the fits using the distributions of ρ shown in the following panels. (b and e): The $P(\rho)$ distributions calculated as described in the text for 50 discrete values of ρ equally spaced in the [0,1] interval. The temperature labeling was omitted for clarity (same color code as in the other panels). The insets show the low ρ region of the plots with appropriate scaling. (c and f): The distributions of panels b and e were converted into a distribution of $\log(k_{AB})$, as explained in the text. Notice that the horizontal spacing between the points is now uneven and that the extreme values for ρ close to 0 or 1 of the $P(\rho)$ distribution are truncated in this representation.

second one is more approximate: depending on temperature and medium (low or high glycerol) the amount of $P^+Q_B^-$ recombination is 5−10%. We will discuss later the impact of $P^+Q_B^-$ recombination on the Y_n kinetics, noticing that it must be minor because the increase of Δt to 400 ms had almost no effect. The question now is can we carry out an inversion of eq 3 and obtain the shape of the $P(\rho,T)$ distribution? This is clearly an "ill-posed" problem (see chapter 18 in ref 33), where one seeks to reconstruct a whole function from a finite number of discrete values. One can however cut up the [0,1] interval allowed for values of ρ into N bins and replace eq 3 by

$$F(n) = \sum_{i=0}^{N-1} P_i\, y(n, \rho_i)$$
$$\rho_i = \frac{i}{N-1};\ P_i \approx \frac{P(\rho_i)}{N} \qquad (4)$$

The problem is then to determine the P_i values that minimize the evaluation function:

$$\sum_{n=1}^{M} \left(Y_n - \sum_{i=0}^{N-1} P_i\, y(n, \rho_i) \right)^2 \qquad (5)$$

where Y_n stands for the experimental data, and M, for the number of flashes. The procedure must incorporate the constraint that the P_i are positive and their sum is equal to 1. We obtained satisfactory solutions using the Levenberg−Marquardt routine of Mathcad. By satisfactory, we mean that the quality of the adjustment was quite good (see the top panels in Figure 8), while the overall shape of the fitted distribution was little dependent on the number of bins adopted (e.g., 25 or 50) and reproducible when analyzing independent experiments. We also ran the minimization routine together with an entropy maximization constraint, weighted by an adjustable Lagrange multiplier.[33] This did not significantly affect the outcome,

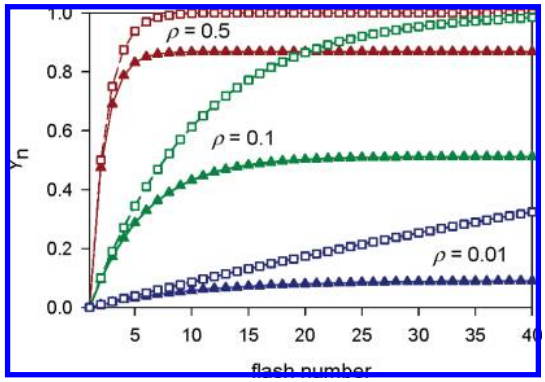

Figure 9. Computed curves, showing the expected incidence of $P^+Q_B^-$ recombination on the Y_n pattern, for various values of ρ, as indicated. The open squares show the patterns in the absence of recombination, using eq 2. The effect of recombination (closed triangles) was taken into account in the following way. An interval of 200 ms between flashes was assumed. We denote as d the fraction of RCs which have not recombined over this time interval ($d = 0.905$ was determined from the decay kinetics after one flash). Denoting as Y_n the fraction of $P^+Q_B^-$ present 200 ms after flash n, immediately before firing flash $n + 1$, the series of the Y_n was computed from the recurrence relation $Y_n = d[Y_{n-1} + \rho(1 - Y_{n-1})]$.

as long as the weighting parameter allowed the evaluator of eq 5 to adopt reasonably small values (so that the χ^2 remains in a plausible range). The distributions obtained from this procedure are shown in Figure 8. The left- and right-hand parts of the figure show results from low and high glycerol experiments, respectively, for temperatures in the −30 to −60 °C region. The top panels show the experimental Y_n values and their fits. Panels b and e show the corresponding distributions of ρ. The results can be summarized as follows. One has first a massif sloping down from the $\rho = 1$ edge; when decreasing the temperature, this massif broadens, its height as well as its integral decreases (thus the height decrease is not just a consequence of broadening). On the other side of the ρ domain, a fraction of RCs is present in the bin located at $\rho = 0$ (i.e., in the [0, 0.01] interval). This fraction increases when lowering T. A third feature is also present, although its robustness is less secure: at −35 °C, a low peak of the distribution appears around $\rho \approx 0.1$, which seems shifted to lower values of ρ at −40 °C. One may speculate that the population of the $\rho = 0$ bin is actually essentially due to the low ρ edge of this bell-shaped curve. In other words, there may not be three features, but only two, i.e., the $\rho = 1$ massif and a low ρ band, which is shifted to lower ρ as T decreases and is responsible for the fraction of RCs collected into the leftmost bin.

One can convert the $P(\rho)$ distribution into a distribution of k_{AB} or, more practically, of $\log(k_{AB})$. Using eq 1, each ρ_i corresponds to a value L_i of $\log(k_{AB})$ such that

$$L_i = \log(k_{AP}) - \log\left(\frac{1}{\rho_i} - 1\right) \tag{6}$$

and the distribution of L is

$$Q_i = Q(L_i) = P(\rho_i)\left|\frac{d\rho}{dL}\right| = P(\rho_i)\ \rho_i(1 - \rho_i)\ \ln(10) \tag{7}$$

The outcome is shown in Figure 8c and f. In this representation, the massif rising to $\rho = 1$ now appears as a bell-shaped curve, which shifts to the left and broadens slightly as the temperature decreases. The low ρ band found in the −30 or −35 °C distributions is enhanced in this representation. The RC population present in the $\rho = 0$ bin in the $P(\rho)$ distribution does not appear as such in the $Q(L)$ distribution (because the corresponding value of L is $-\infty$) but corresponds to the area extending from the leftmost point. Similarly the $P(1)$ value of the ρ distribution measures the area truncated on the right-hand side of the $Q(L)$ distribution.

The families of distributions obtained when varying T in the low or high glycerol media are roughly similar. The plots of $\langle\rho\rangle$ as a function of T (Figure 5) showed no clear effect of the solvent. Nevertheless, the Y_n patterns are significantly different in the two media: for instance, in the high glycerol medium, the increment on the second flash is larger and so is the overall amplitude of the rise over 30 flashes. This means that the region with intermediate ρ values is more populated in this medium, as indeed found in the deconvoluted distributions. The broadening of the distribution seems to occur earlier (i.e., at higher temperatures) in the high glycerol medium. In this respect the splitting observed at −60 °C in the high glycerol medium may be anticipating a similar change that would occur at lower T in the low glycerol medium.

Postrecombination Memory of the $P^+Q_B^-$ State. The fact that the Y_n pattern depends only on n, and not on the time spacing between flashes (at least in the 100−400 ms range), was a strong argument in favor of a "frozen landscape" picture, because it proves that the accumulation of $P^+Q_B^-$ is not controlled by conformational relaxation. However, as already noticed, the extent of $P^+Q_B^-$ recombination that takes place during a 400 ms interval is significant (e.g., in the low glycerol medium at −50 °C, the overall $t_{1/2}$ is ∼1.5 s); furthermore, during a train of 30 flashes, the amount of RCs that have turned over several times between the ground and $P^+Q_B^-$ states is quite different depending on whether the overall duration is 3 or 12 s. However, as argued below, quite significant effects are expected when varying the Δt in this range, *unless* a specific ingredient is added to the frozen landscape model.

Figure 9 shows simulations computed for $y(n,\rho)$ when the effect of recombination is either ignored or taken into account. As may be seen, the effect, computed here for $\Delta t = 200$ ms, is quite significant (especially for low values of ρ). When varying the Δt, the simulations predict modifications of the Y_n pattern that are greatly above the experimental accuracy. The assumption made here is that the RCs which recombine from $P^+Q_B^-$ to the ground state remain in the same bin of the $P(\rho)$ histogram, retaining the same probability to form $P^+Q_B^-$ as in the dark-adapted state. Thus, RCs with a low ρ will on average require many attempts before reaching the $P^+Q_B^-$ state; if recombination implies a return to square one, this means starting the process all over again, and this is the reason for the sensitivity to recombination appearing in these simulations.

The observed insensitivity of the Y_n pattern to the Δt between flashes implies that the above assumption (i.e., recombination restores the dark-adapted ρ distribution) must somehow be called into question. The results actually suggest that the RCs which have just recombined are endowed with a high yield for producing Q_B^- ($\rho \approx 1$), so that the next flash essentially returns them back to $P^+Q_B^-$. Two possibilities may then be envisaged: either RCs with a high ρ recombine faster, causing a temporary enrichment in this type of centers or the passage through the $P^+Q_B^-$ state produces a conversion of all RCs to a high ρ character. The first possibility, implying a slower recombination rate of RCs with a small ρ, would make sense, because a low ρ implies a small k_{AB} rate and thus, for a given ΔG_{AB}, also a slow backward rate constant (k_{BA}), resulting in slow recombination. To test

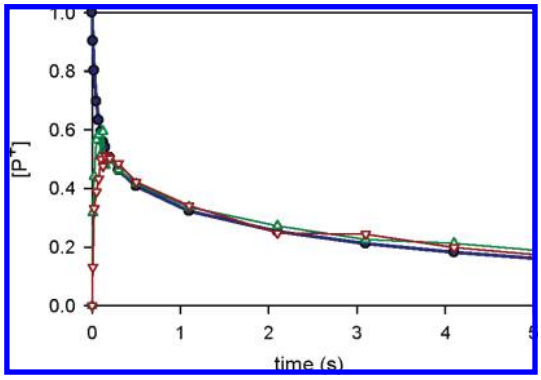

Figure 10. A comparison of the decay kinetics after one, two, or three flashes. The dark-blue full circles and line show the time course of P^+ after one saturating flash (denoted as 1F in the text). The open green triangles show the difference 2F−1F between the kinetics following two flashes (separated by 100 ms) and one flash, with an arbitrary ×14 magnification for comparison with 1F. The open brown triangles show the difference 3F−2F, with magnification ×38. The experiment was run at −50 °C in the low glycerol medium.

this possibility, we compare (Figure 10) the recombination kinetics after one (1F), two (2F), or three (3F) flashes separated by 100 ms. The difference 2F−1F displays the recombination of the RCs that were converted to $P^+Q_B^-$ by the second flash. This corresponds to a population of RCs with a much smaller ρ, compared with the $P^+Q_B^-$ formed on the first flash. Indeed, at −50 °C, the average ρ in the dark-adapted state ($\langle\rho\rangle = Y_1$) is 0.58, while the RCs that are open immediately before firing the second flash have an average ρ of 0.041 (given by $Y_2 - Y_1$). Similarly the population of open RCs before the third flash has an average ρ of 0.015. Despite this drastic change regarding ρ, the kinetics of the differences 2F−1F or 3F−2F are similar to the recombination kinetics after flash 1. This excludes the interpretation implying that the recombination might select RCs with a large ρ and supports the alternative possibility that RCs converted to $P^+Q_B^-$ acquire a high ρ character, which they can retain at least for some time after they have recombined (a "memory" of the passage through the $P^+Q_B^-$ state). This hypothesis is reminiscent of the effect described by Kleinfeld and co-workers:[34] when RCs are cooled at 77 K in the dark, they are trapped in a state unable to reduce Q_B (the temperature dependence shown in Figure 5 results in $\langle\rho\rangle = 0$ at 77 K). However, if the material is illuminated during the cooling process (thus kept in the $P^+Q_B^-$ state and then allowed to recombine at 77 K), the RCs are now trapped in a state with $\rho \approx 1$ (the yield of $P^+Q_B^-$ formed by one flash was found ≥0.98). The authors suggested that this could be explained by the trapping of a proton in the neighborhood of Q_B. An alternative explanation was later put forward by Stowell and co-workers,[14] involving the trapping of Q_B in a "proximal" position.

A direct test of the memory effect proposed above is to measure the value of ρ after a train of flashes accumulating a substantial amount of $P^+Q_B^-$ followed by a dark interval allowing significant recombination of the RCs. One can compare in this manner the predictions of the extreme cases where the recombining RCs either retain their original ρ (case 1) or acquire a $\rho \approx 1$ property (case 2). We use the following notations (see Figure 11a): $Y_1 = \langle\rho\rangle$ is the amount of $P^+Q_B^-$ formed by the first flash; Y_N is the amount of $P^+Q_B^-$ accumulated after flash N, at the end of the preillumination train; Y_D is the level reached at the end of the recombination period, immediately before firing the test flash; Y_{N1} is the level reached after firing the test flash. The prediction of case 2 for the value of Y_N is simply that $Y_{N1}(2) \approx Y_N$ (the 2 in parentheses means: "for case 2"; this expression neglects the small increment that would be induced by flash $N + 1$ if the sequence had been pursued). The prediction of case 1 is that the fraction $(Y_N - Y_D)/Y_N$ of RCs which have recombined should behave as dark-adapted RCs, with an average $\langle\rho\rangle$ given by Y_1. Thus, one expects

$$Y_{N1}(1) = Y_D + Y_1\frac{Y_N - Y_D}{Y_N} \tag{8}$$

(again neglecting the increment on flash $N + 1$ in a regular sequence). The experimental result (see the inset of Figure 11a) is located between the values predicted by the two models, suggesting that the memory effect does occur but is progressively erased. This is substantiated by the plot of panel b, which shows the relative location of the experimental Y_{N1} between the values $Y_{N1}(1)$ and $Y_{N1}(2)$ predicted by the two models. In the low glycerol medium, the erasure process is multiphasic (the data were fitted by a sum of two exponentials), with an overall $t_{1/2} \approx 3$ s at −40 °C. This is consistent with the fact that, over a sufficiently short interval (e.g., $\Delta t \leq 400$ ms), the centers that recombine are essentially in a state with $\rho \approx 1$, accounting for the insensitivity of the Y_n pattern to Δt. On the other hand, the memory erasure kinetics were much faster and apparently more homogeneous in the high glycerol medium, which is consistent with the greater sensitivity of the Y_n pattern to Δt (i.e., the clipping of the slowest phases mentioned when discussing Figure 7b).

We also investigated the memory erasure process using a procedure similar to that of Kleinfeld et al.[34] In the experiment of Figure 11c, the chromatophores were cooled from −15 to −50 °C under 875 nm illumination (the cooling/illumination duration was 60 s). When switching off the 875 nm light, the recombination kinetics at −50 °C were markedly slower ($t_{1/2} \approx 8$ s) than the $P^+Q_B^-$ recombination after one flash on a dark-adapted sample ($t_{1/2} \approx 2$ s). This effect is due to the long illumination maintaining the RCs in the $P^+Q_B^-$ state and allowing them to reach increasingly stabilized conformations, as further discussed below. A saturating flash was fired at various times after switching off the 875 nm DC light, and the kinetics were analyzed by subtracting the background decay recorded in the absence of the flash. The increasing relative amplitude of the fast phase when increasing the delay is indicative of the recovery rate from the initial "Kleinfeld state" with $\rho = 1$ to the dark-adapted state with an average $\langle\rho\rangle \approx 0.5$. The half-time for this process is ∼8 s. It is slower than that found in the procedure of panels a and b, using a multiflash preillumination at a fixed temperature, which is probably due to the deeper stabilization of $P^+Q_B^-$ occurring under the 60 s cooling/illumination procedure. The relaxation of the "Kleinfeld state" was previously studied[28] in isolated RCs of *Rb. sphaeroides* in a procedure involving cooling under illumination down to 77 K (where the RCs are let recombine) and then testing the memory relaxation when raising the tem-

(33) Press, W. H.; Flannery, B. P. ; Teukolsky, S. A.; Vetterling, W. T. *Numerical recipes in C: the art of scientific computing*; Cambridge University Press: 1992.
(34) Kleinfeld, D.; Okamura, M. Y.; Feher, G. *Biochemistry* **1984**, *23*, 5780–5786.

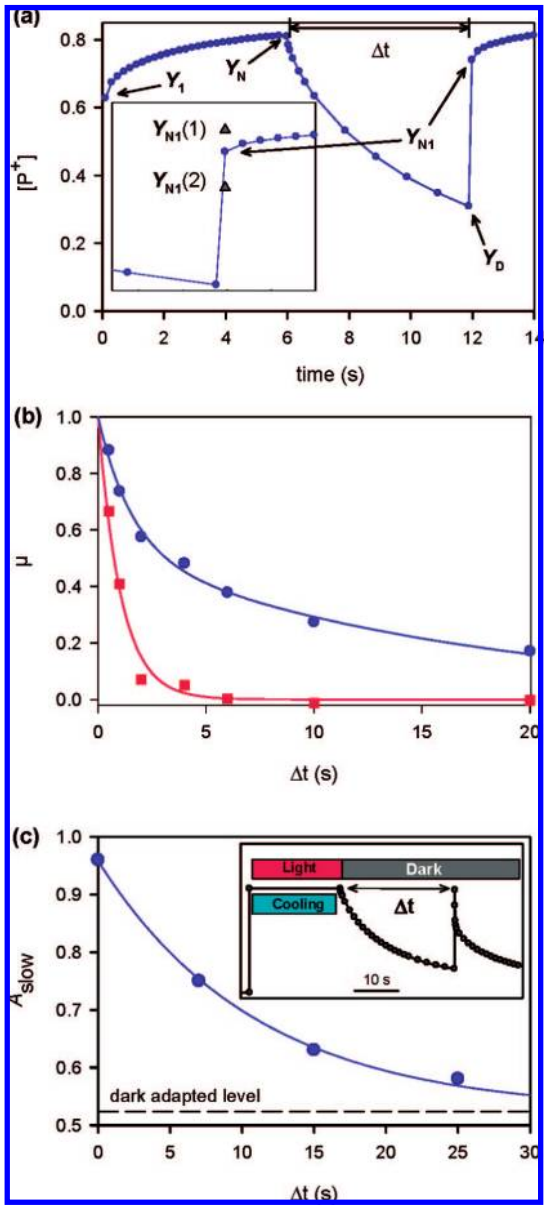

Figure 11. Investigation of the "post-recombination memory" of the $P^+Q_B^-$ state. (a and b) The chromatophores were subjected to a series of 30 actinic flashes (with 200 ms spacing) at −40 °C, allowing a significant accumulation of $P^+Q_B^-$. The flash train was then interrupted and resumed after a dark period Δt. (a) A typical record, with data points sampled 100 ms after each flash, illustrating the notations defined in the text. The inset is a zoom on the beginning of the second flash train, showing the location of the measured Y_{N1} between the computed values $Y_{N1}(1)$ and $Y_{N1}(2)$, corresponding respectively to 100% and 0% memory effect, respectively. (b) A plot of parameter $\mu = (Y_{N1}(2) - Y_{N1})/(Y_{N1}(2) - Y_{N1}(1))$, which characterizes the location of the experimental data point between $Y_{N1}(1)$ and $Y_{N1}(2)$, as a function of Δt, with blue and red symbols for the low and high glycerol media. (c) Chromatophores suspended in the low glycerol medium where cooled from −15 °C down to −50 °C under a saturating continuous 875 nm illumination. When reaching −50 °C (i.e., 1 min after starting illumination and cooling) the light was turned off. The decay kinetics were recorded, and a test flash was fired at variable times Δt after switching the light off. The inset illustrates a typical experiment (with here $\Delta t = 25$ s; the duration of the light/cooling phase is not on scale), showing the absence of a fast recombination phase after the continuous illumination period (all RCs are in the $P^+Q_B^-$ state) and its partial recovery in the kinetics following the flash, reflecting the gradual return to the dark-adapted value of $\langle\rho\rangle$. The main panel shows the relative extent of the slow phase as a function of Δt (this was determined from the difference traces between the flash-induced kinetics and the background decay measured separately). The dashed line shows the dark-adapted level.

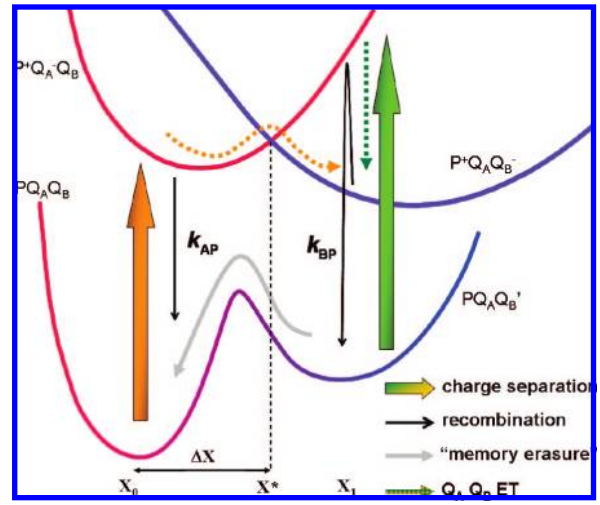

Figure 12. A scheme illustrating the interpretations proposed in the text. The curves depict the energy landscape for the various states of the RC, considering the RCs belonging to a particular "ρ bin". The conformational coordinate X describes the rearrangements caused by charge separation and by the Q_A to Q_B electron transfer. The dark-adapted system is found predominantly at X_0. A flash (orange vertical arrow) promotes the RC to the $P^+Q_A^-$ curve, where the ET step to Q_B is initially uphill. The value of ρ depends on the competition between recombination (k_{AP}) and the rate for drifting to X*, where ET to Q_B becomes downhill. When the $P^+Q_AQ_B^-$ state is formed, it continues its stabilization process, which, at low temperature, may (high glycerol case or prolonged illumination in the low glycerol medium) or may not (low glycerol medium) reach completion before recombination takes place. Recombination of $P^+Q_AQ_B^-$ (the k_{BP} arrow is meant for both the direct and indirect pathways described in Figure 2) occurs at some X_1 value, from which the RC drifts back to the more stable conformation at X_0 (gray pathway). If a flash is fired at a short time after recombination (green vertical arrow), the RC is still in a conformation PQ_AQ_B' where the ET to Q_B is downhill (dashed green arrow), ensuring $\rho \approx 1$. Since the conformational redistribution of the "ρ bins" appears frozen, a second conformational coordinate Y (not shown) is required to describe the extremely rugged landscape accounting for this situation.

perature. The highest temperature in this study was 200 K, but using the Arrhenius parameters reported by the authors, one can extrapolate a rate of 0.02 s^{-1} at −50 °C (or $t_{1/2} \approx$ 31 s). This is reasonably close to our own estimate ($t_{1/2} \approx$ 8 s), considering the differences in biological material and experimental procedure.

Discussion

Frozen Landscape vs Conformational Equilibrium. The diminished extent of Q_B^- formed by a single flash at low temperature was previously ascribed to the slowing of the $Q_A^-Q_B \rightarrow Q_AQ_B^-$ reaction, assuming that that the dispersion of the rate constant could be neglected.[28] We found, however, that the pattern of $P^+Q_B^-$ accumulation when the chromatophores were submitted to a train of saturating flashes was clearly at odds with a homogeneous model, showing that the reaction centers were distributed among heterogeneous states with very different yields ρ for $P^+Q_B^-$ formation. Two types of models may account for this heterogeneous distribution. A first possibility is a temperature-dependent equilibrium between two or more conformations, with "passing" (large ρ) or "blocking" (low ρ) character. If the blocking conformation has both a lower enthalpy and lower entropy than those of the passing one, the equilibrium will be in favor of the passing conformation at high T and of the blocking one at low T. This model implies a dynamic interconversion between

the various forms. We found no equilibration delay when changing the temperature as fast as allowed by our setup, which implies that the interconversion rate in this model should be faster than $\sim(20\ s)^{-1}$. An alternative possibility is that the heterogeneous conformation distribution is essentially static, frozen in the subzero temperature range. In this case, the effects observed when lowering the temperature must reflect the response to temperature of a fixed range of conformations. For instance, if the conformational distribution corresponds to a range of activation enthalpies for the $Q_A^-Q_B \rightarrow Q_AQ_B^-$ reaction, the $\rho = 0.5$ boundary will move to conformations with smaller activation enthalpies as the temperature is decreased. In order to discriminate between these models, we examined the kinetics of $P^+Q_B^-$ accumulation under continuous illumination or flashing light. As argued below, the results support the frozen landscape picture. We shall later slightly qualify this view and suggest that some temperature-dependent conformational change may also be involved.

The equilibrium model predicts the accumulation of $P^+Q_B^-$ under prolonged illumination, with a rate reflecting the equilibrium relaxation (provided the illumination intensity is sufficient to keep the passing centers in the $P^+Q_B^-$ state). This statement remains valid for the different variants of the model, e.g., depending on whether one authorizes the passing/blocking relaxation in the charge-separated states as well as in the ground state and, if this relaxation is allowed, depending on the fate assumed for $P^+Q_B^-$ when switching to the blocking conformation (in the particular case when the relaxation proceeds with unmodified rates in the charge separated state and when the conversion of the passing $P^+Q_B^-$ state to the blocking conformation entails the formation of $P^+Q_A^-$, the illumination would cause no accumulation of $P^+Q_B^-$). We thus examined the kinetics of $P^+Q_B^-$ accumulation under light, to determine the relaxation rate of the putative equilibrium between the passing/blocking conformations. We found, however, that this process did not show the rate-limitation expected for a "dark" relaxation but was indicative of photochemical control. We observed a dependence of the pattern of Q_B^- accumulation with the number of saturating flashes, irrespective of the time interval between flashes (100−400 ms). This precludes the occurrence of a significant relaxation of the conformational equilibrium over a time range ≥ 10 s. We attempted to obtain an estimate of the time range where the relaxation of the "frozen landscape" occurs, by searching evidence for a slow phase of $P^+Q_B^-$ accumulation under saturating illumination. Such a slow phase would reflect the rate at which the RCs can escape the conformations with $\rho \approx 0$. At −50 °C, we observed a rise with $t_{1/2} \approx 12$ s, which is probably still due to the photochemical process, but we could not resolve a significant rise reflecting conformational relaxation over illuminations of several minutes.

***P*(ρ) Distribution.** The accumulation of $P^+Q_B^-$ under a flash train is consistent with the stochastic process whereby each RC has a given probability ρ to produce state $P^+Q_B^-$ upon a flash. The observed pattern can then be analyzed to retrieve the distribution of ρ among the RCs. There is not a strictly unique distribution corresponding to a given experimental sequence, but our experience with various fitting and simulation procedures has suggested that the problem is not too ill-conditioned and that the shape of the distribution is fairly well determined. A major feature emerging from this analysis is that the distribution of ρ and, thus, of the effective k_{AB} rate, is quite broad. For instance, at −50 °C, using the ρ histograms of Figure 8b (low glycerol medium), 23% of the RCs have $k_{AB} > 400\ s^{-1}$ ($t_{1/2} \leq 1.7$ ms), while 20% has $k_{AB} < 0.21\ s^{-1}$ ($t_{1/2} > 3.4$ s). Furthermore, the experiment of Figure 7c shows that more than 10% of the RCs are actually blocked over time ranges of several minutes. The occurrence of a broadening of the k_{AB} distribution in isolated RCs of *Rb. sphaeroides* was previously reported by Tiede et al.[32] as soon as −22 °C was reached. The distribution of k_{AB}, or $\ln(k_{AB})$, resulting from this analysis, is clearly multimodal. In Figure 8c and f, there is, on the high rate side, a bell-shaped distribution (in the $\ln(k_{AB})$ plot). The largest part of the RCs belong to this band, but this population decreases when lowering *T*. This is accompanied by an increased separate population of RCs with small k_{AB}. Before examining further the temperature dependence of $P(\rho)$, we would like to discuss the origin of the rate modulation.

Nature of the Conformational Control on ρ. As discussed above, this control covers more than 3 orders of magnitude (much more, actually, if one takes into account the fraction of RCs with k_{AB} blocked over several minutes of saturating illumination). One may list three ways by which the protein conformation can modulate the rate of Q_B reduction. (i) The effect pertains to the activation energy for electron transfer, i.e., to the exponent $(\Delta G_{AB} - \lambda)^2/4\lambda$ in the Marcus formula, where λ is the reorganization energy. (ii) It may be a matter of distance between both partners. The Stowell model[14] where the Q_B quinone can move from a distal to proximal position relates to this case (the ∼4.5 Å change in distance with respect to Q_A is expected to affect the rate by 2 to 3 orders of magnitude). (iii) The modulation may not be primarily a matter of electron transfer rate constant but rather reflect the stabilization of Q_B^-. Considering possibility (i), it seems dubious that the protein might change the reorganization energy over a range affecting the ET rate by more than 3 orders of magnitude. On the other hand, if the modulation arises from ΔG_{AB}, the required amount of slowing implies that the reaction enters far into the endergonic region, which actually puts case (iii) at the forefront. The distance distribution hypothesis (case ii) appears compatible with our results. We note, however, that serious objections have been raised against the Stowell hypothesis as an explanation for the conformational gating of the $Q_A^-Q_B \rightarrow Q_AQ_B^-$ reaction.[35–38] In particular, it has been argued that the IR spectra indicate that, under functional conditions, Q_B is essentially bound at the proximal site in the dark-adapted state.[35,37] Although we cannot exclude case (ii), we believe that the stabilization hypothesis, case (iii), is more plausible. A scheme illustrating this model is shown in Figure 12. When the $P^+Q_A^-Q_B$ state is formed, the ET from Q_A to Q_B is initially uphill ($\Delta G_{AB} > 0$). Thus, the ET equilibrium between the two partners may be rapid, but the electron remains mostly on Q_A at this stage. The system then relaxes toward configurations where the stabilization of the electron on Q_B becomes increasingly favorable ($\Delta G_{AB} < 0$). The effective rate constant k_{AB} in this case reflects the rate of this stabilization process, rather

(35) Breton, J. *Biochemistry* **2004**, *43*, 3318–3326.
(36) Kuglstatter, A.; Ermler, U.; Michel, H.; Baciou, L.; Fritzsch, G. *Biochemistry* **2001**, *40*, 4253–4260.
(37) Breton, J.; Boullais, C.; Mioskowski, C.; Sebban, P.; Baciou, L.; Nabedryk, E. *Biochemistry* **2002**, *41*, 12921–12927.
(38) Xu, Q.; Baciou, L.; Sebban, P.; Gunner, M. R. *Biochemistry* **2002**, *41*, 10021–10025.

than a bona fide ET rate constant. Similar interpretations of the gating mechanism have been proposed previously.[11,13] One reason for favoring this model is that, as argued below, our low temperature data give several indications that the degree of Q_B^- stabilization with respect to Q_A is a flexible parameter capable of undergoing significant modifications over a few seconds.

Q_B^- Stabilization and Effects of Glycerol. A first evidence for a conformational change associated with the stabilization of the $Q_AQ_B^-$ state is the phenomenon that we designated as a post-recombination memory: RCs that were initially in a configuration with a low ρ value, so that their photoconversion to $P^+Q_AQ_B^-$ required many turnovers, appear as efficient, high ρ centers at short times after their recombination to state PQ_AQ_B. This memory does not last very long, and the initial distribution is eventually recovered. We believe this phenomenon has the same origin as that discovered by Kleinfeld and co-workers[34] for the effect of cooling to cryogenic temperature under illumination, which results in trapping the RC into a state with $\rho \approx 1$. In our case, the intermediate temperature range allows both the trapping and detrapping to take place at the same temperature, with measurable time responses.

The mechanism that we propose is illustrated in Figure 12: the conformational coordinate "X" controlling the value of ΔG_{AB} is not modified when the recombination takes place, so that a new charge separation finds initially the RCs in the appropriate conformation for a high ρ. We found that the relaxation to the dark-adapted state (memory erasure) was faster and more homogeneous in the high glycerol medium (Figure 11b). Similar effects of glycerol were also apparent for the $P^+Q_AQ_B^-$ recombination kinetics (Figure 4b). Below -20 °C, in the low glycerol medium, these kinetics became faster when decreasing T, and their heterogeneity became more pronounced. This is easily understood by assuming that the stabilization process is slow and cannot reach completion in a fraction of the RCs, before recombination takes place. This means a less negative ΔG_{AB} and, consequently, a faster recombination rate. In agreement with this interpretation, the recombination kinetics became slower when the RCs were submitted to a prolonged illumination (i.e., for 10 s), which maintained the RCs in the $P^+Q_AQ_B^-$ state and allowed them to reach more stabilized configurations. In the high glycerol medium, the recombination kinetics were more homogeneous and slower and showed a normal Arrhenius (or van't Hoff) temperature dependence until the direct pathway became predominant. Similarly, in this medium, the kinetics were not further slowed down when the sample was submitted to a strong continuous illumination for several tens of seconds. Therefore, an effect of the cryoprotecting high glycerol medium, maintaining a viscous but fluid matrix, is to facilitate the movements along the conformational coordinate that we denote as X, i.e., the changes that are responsible for the stabilization of state $P^+Q_AQ_B^-$. The anomalous acceleration of $P^+Q_AQ_B^-$ recombination at low temperatures in the low glycerol medium appears below -20 °C and, thus, is not simply correlated with the freezing of the aqueous matrix. We actually obtained evidence[39] that a layer of liquid medium is still present around the membrane-associated RCs down to -40 °C.

Frozen and Dynamic Features at Subzero Temperatures. To explain our results, we need, in addition to X, another conformational coordinate, Y, which is required to characterize the "frozen" (on a time range ≤ 10 s) distribution of ρ. The scheme of Figure 12 is meant to describe the events occurring to the fraction of RCs with some definite value of ρ (belonging to some "ρ bin"). We may assume that this value of ρ is determined by the distance denoted as ΔX on the scheme, i.e., the distance along coordinate X between the initial, dark-adapted conformation X_0 and X*, the conformation where the transition becomes downhill. If, for instance, $\rho = 0.5$, the time required to drift over the distance ΔX is approximately k_{AP}^{-1} (≈ 50 ms). Coordinate Y is intended to characterize the conformational feature that controls ΔX. The energy profile along coordinate Y must be very rugged, with high barriers accounting for the slow relaxation time, i.e., tens of seconds to minutes. What is the significance of the X and Y coordinates? A plausible interpretation, following Kleinfeld et al.,[34] is that the stabilization process mapped by X represents the movement of a proton toward a binding site approaching Q_B^-. The distance ΔX may then characterize the rate at which a proton can move to the appropriate location, depending on its site of origin and the conductance of the channel that it takes. Both features may be controlled by fine details of the protein conformation, e.g., modulating the structure of the hydrogen bond network or of a protonated water structure (see the recent review by Wraight,[40] the discussion by Cheap et al.,[41] and references therein): this would account for coordinate Y. The involvement of a proton movement in the stabilization process that determines ρ is consistent with the effect of pH investigated by Xu and Gunner.[42] The temperature dependence of $\langle\rho\rangle$ (i.e., the amount of $P^+Q_B^-$ produced by one flash) was not modified in the pH range 6−8 but did vary at higher pH, where the decrease of $\langle\rho\rangle$ was shifted toward higher T. The results suggest that the proton required to stabilize Q_B^- is initially located on a group with $pK_a \approx 9.5$. At high pH, when this group is not protonated in the dark-adapted state, the stabilization process is hindered.

Temperature Dependence of the Conformational Distribution. According to the frozen landscape picture, the effect of T on the $P(\rho)$ distribution should reflect the temperature response of a fixed conformational distribution. Considering for instance a bell-shaped distribution of activation enthalpies, the $P(\rho)$ distribution and its temperature dependence could then be generated by applying an Arrhenius law (or transition state theory) to this distribution. Qualitatively, this approach predicts a distorted, but gradual, shift of the distribution "to the left" when lowering T. This behavior was indeed observed for the high rate feature of the distribution, i.e., the "massif" at $\rho > 0.6$ (or, for the $\ln(k_{AB})$ distribution, the bell-shaped band at $\ln(k_{AB}) > 1$). When analyzed in this manner, the temperature dependence of the peak would correspond to activation enthalpies of ~174 meV (17 kJ/mol) in the low glycerol medium and 213 meV (20 kJ/mol) in the high glycerol medium (these are very rough estimates due to the poor quality of the Arrhenius plots). The corresponding extrapolated rate at room temperature would be ~1300 s^{-1} ($t_{1/2} \approx 500\ \mu s$) in both cases. The observed

(39) Ginet N.; Comayras, F.; Lavergne, J. In *Photosynthesis: Fundamental Aspects to Global Perspectives*; van der Est, A. , Bruce, D., Eds.; Allen Press: Lawrence, KS, 2005; Vol. 1, pp. 204−207.

(40) Wraight, C. A. *Biochim. Biophys. Acta* **2006**, *1757*, 886–912.

(41) Cheap, H.; Julia Tandori, J.; Derrien, V.; Benoit, M.; de Oliveira, P.; Koepke, J.; Lavergne, J.; Maroti, P.; Sebban, P. *Biochemistry* **2007**, *46*, 4510–4521.

(42) Xu, Q.; Gunner, M. R. *Biochemistry* **2002**, *41*, 2694–2701.

rate on this material is actually ~20-fold faster ($k_{AB} \approx 2.3 \times 10^4$ s^{-1}), consistent with a rapid drift along the Y coordinate above 0 °C.

However, in addition to this Arrhenius type of behavior, one observes a depletion of the high rate band when lowering T, accompanied by an increased population of RCs with small k_{AB}. In the frozen low glycerol medium, a single feature may suffice to describe the low rate population. It appears first as a bell-shaped distribution (around $\ln(k_{AB}) \approx 0.6$ at −30 °C); when lowering T, the curve undergoes a drastic broadening and displacement toward lower rates. The same description applies to the data from the 66% glycerol medium, but an additional splitting of the high rate band appears in the −55 and −60 °C distributions. Irrespective of these details, one has clearly an accumulation of quasi blocked RCs at low temperature (evidenced as an increased population of the $\rho \approx 0$ bin in Figure 8b and e).

The description proposed above of a conformational landscape frozen along coordinate Y may not be sufficient to account for this complex temperature dependence. We believe that the depletion of the high rate band and accumulation of blocked RCs arises from an additional conformational modification depending on temperature. However, if a temperature-dependent conformational equilibrium is involved, one expects dynamic effects showing the occurrence of a relaxation when changing the external parameters (illumination or temperature). We did not succeed in this search, though. The flash experiments indicated that no significant relaxation occurs in the 10 s time range; the test using continuous saturating illumination pushed the limit further into the minutes range. Yet, we could not resolve a significant delay for the response upon one flash (measuring $\langle\rho\rangle$) when changing rapidly (15−20 s) the temperature of the sample from −50 to −60 °C. Clearly, according to our analysis, part of the change of $\langle\rho\rangle$ with temperature can be ascribed to the "Arrhenius-type" response, which reacts instantaneously to the temperature change, but the contribution we ascribe to a modification of the conformational distribution should also be significant.

We are thus faced with the difficulty that the increasing population of RCs with $\rho \approx 0$ when cooling the system seems to imply a temperature-dependent conformational evolution, whereas we failed to detect the associated kinetic relaxation. A possible explanation is that we do not detect RCs escaping from the "$\rho = 0$ bin" under prolonged illumination because, for these RCs, the conformational equilibrium constant is largely in favor of a $\rho \approx 0$ conformation. This interpretation would imply the following requirements. First, the equilibrium involving the $\rho \approx 0$ conformation should have a steep temperature dependence (implying that the transition to the blocked conformation involves large enthalpic and entropic changes, possibly due to a cooperative rearrangement[43]); second, the parameters controlling the transition temperature should be broadly distributed, so that the swing to the $\rho \approx 0$ conformation occurs gradually over the whole RC population; and, third, the time constant for the conformational switch responding to a temperature change should be shorter than ~15 s. Due to these features, the fraction of RCs for which the conformational equilibrium constant K_{eq} is close to 1 at some given temperature can be small, while most of the other RCs have either $K_{eq} \ll 1$ or $K_{eq} \gg 1$. This can account for the negative result of the experiment using continuous illumination to displace RCs from the "$\rho = 0$ bin", which can only detect RCs which are not too deeply stabilized in the blocked conformation (otherwise the "off-rate" would be too small).

Conclusion

The present results are reminiscent of those obtained with the chloroplasts photosystem I RC from chloroplasts at low temperature.[1] In this system also, evidence was reported for a broad frozen conformational distribution controlling the yield of electron transfer to the terminal Fe−S cluster acceptor F_{AB}, in competition with charge recombination.[44,45] In this case, however, the conformational freezing occurred at ~170 K,[46] well below the temperature range explored in the present study. The freezing of protein conformations ("glass transition") is commonly observed at ~170−220 K[16,46–49] and generally ascribed to the glass transition of the solvent (analogous to our high glycerol medium in most cases). In the present work, a drastic slowing down of the conformational relaxation (along "coordinate Y") was observed below −25 °C in a frozen water matrix as well as in the fluid 66% glycerol medium (where the glass transition occurs around 190 K). This "high temperature" (≥250 K) transition has not been observed in previous studies with bacterial RCs. In their work on the conformational control of the $P^+Q_A^-$ recombination in RCs of *Rb. sphaeroides*, McMahon and co-workers[2] estimated the distribution of relaxation rates at various temperatures. Their results suggest that, at −25 °C, the conformational changes that are coupled with $P^+Q_A^-$ recombination relax in less than 100 ms in more than 90% of the RCs. The present work shows that the conformational movements that are responsible for the gating of the $Q_A^-Q_B \rightarrow Q_AQ_B^-$ reaction belong to a different category, with a remarkably high, although not unprecedented, transition temperature.

A similarly high transition temperature has indeed been found in studies of the bacteriorhodopsin cycle in purple membranes. In this system, the decay of state M_2 is drastically slowed down around 260 K. The blocked step is one of the final events in the bacteriorhodopsin cycle, whereby the reprotonation of the Schiff base occurs. This transition appears correlated with important changes affecting the protein and its environment: (i) a dehydration process is occurring, resulting in a narrower space between stacked membranes; (ii) this dehydration is accompanied by a decrease of the amount of large amplitude fluctuations, as revealed by in incoherent neutron scattering experiments.[51] The role of the hydration layers is confirmed by the fact that

(43) Nocek, J. M.; Stemp, E. D. A.; Finnegan, M. G.; Koshy, T. I.; Johnson, M. K.; Margoliash, E.; Grant Mauk, A.; Smith, M.; Hoffman, B. M. *J. Am. Chem. Soc.* **1991**, *113*, 6822–6831.

(44) Crowder, M. S.; Bearden, A. *Biochim. Biophys. Acta* **1983**, *722*, 23–35.

(45) Sétif, P.; Mathis, P.; Vänngård, T. *Biochim. Biophys. Acta* **1984**, *767*, 404–414.

(46) Schlodder, E.; Brettel, K.; Falkenberg, K.; Gergeleit, M. In *Photosynthesis from light to biosphere*; Mathis, P., Ed.; Kluwer Academic Publishers: Dordrecht, 1995; Vol. 2, pp 107−110.

(47) Fenimore, P. W.; Frauenfelder, H.; McMahon, B. H.; Parak, F. G. *Proc. Natl. Acad. Sci. U.S.A.* **2002**, *99*, 16047–16051.

(48) Rasmussen, B. F.; Stock, A. M.; Ringe, D.; Petsko, G. A. *Nature* **1992**, *357*, 423–424.

(49) Vitkup, D.; Ringe, D.; Petsko, G. A.; Karplus, M. *Nat. Struct. Biol.* **2000**, *7*, 34–38.

(50) Rasmussen, D. H.; MacKenzie, A. P. *J. Phys. Chem.* **1971**, *75*, 967–973.

(51) Dencher, N. A.; Sass, J. H.; Büldt, G. *Biochim. Biophys. Acta* **2000**, *1460*, 193–203.

the M_2 state relaxation is also blocked by dehydration of purple membranes at room temperature.

In line with the above results, it is noteworthy that a heterogeneous distribution of ρ, similar to the low temperature effects described in the present work, has been demonstrated at room temperature, in isolated RCs included in a dehydrated trehalose matrix.[52] In these experiments, varying the degree of dehydration produced a similar effect such as temperature lowering. From this discussion, one may propose the following interpretation: large scale fluctuations that require a fully hydrated environment of the RC are responsible for allowing transitions (along "coordinate Y") between conformations which present a broad distribution as regards the rate of stabilization of the Q_B^- state, presumably through proton movements. A dehydration of the membrane, whether due to desiccation in the trehalose treatment or to temperature lowering, suppresses these large scale fluctuations, thus causing the immobilization of the conformational manifold.

Acknowledgment. We thank A. Verméglio for highly valuable advice.

JA076504F

(52) Francia, F.; Palazzo, G.; Mallardi, A.; Cordone, L.; Venturoli, G. *Biochim. Biophys. Acta* **2004**, *1658*, 50–57.